

THE OFFICIAL MAGAZINE OF THE OCEANOGRAPHY SOCIETY

Oceanography

CITATION

Venayagamoorthy, S.K., and O.B. Fringer. 2012. Examining breaking internal waves on a shelf slope using numerical simulations. *Oceanography* 25(2):132–139, <http://dx.doi.org/10.5670/oceanog.2012.48>.

DOI

<http://dx.doi.org/10.5670/oceanog.2012.48>

COPYRIGHT

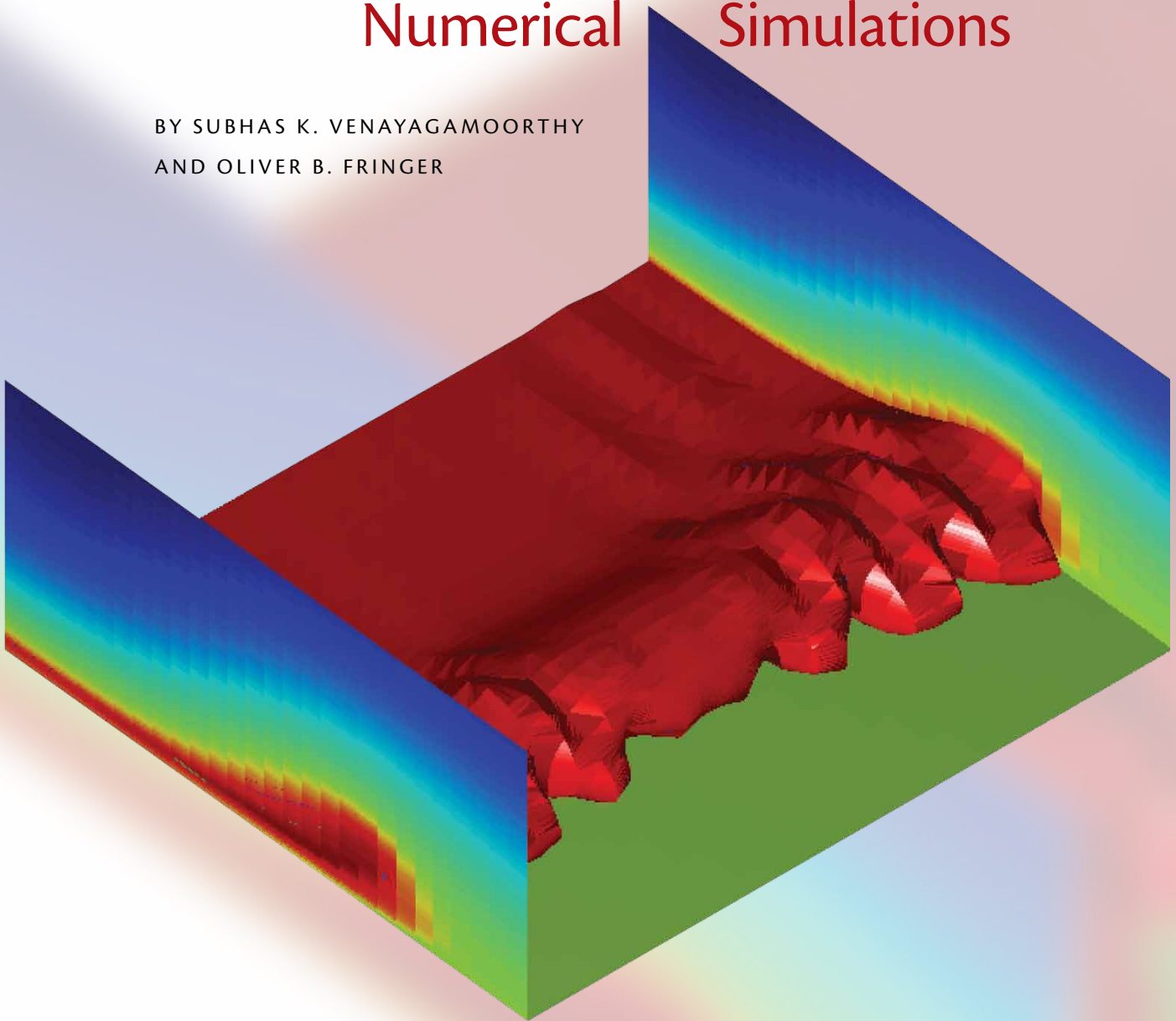
This article has been published in *Oceanography*, Volume 25, Number 2, a quarterly journal of The Oceanography Society. Copyright 2012 by The Oceanography Society. All rights reserved.

USAGE

Permission is granted to copy this article for use in teaching and research. Republication, systematic reproduction, or collective redistribution of any portion of this article by photocopy machine, reposting, or other means is permitted only with the approval of The Oceanography Society. Send all correspondence to: info@tos.org or The Oceanography Society, PO Box 1931, Rockville, MD 20849-1931, USA.

Examining Breaking Internal Waves on a Shelf Slope Using Numerical Simulations

BY SUBHAS K. VENAYAGAMOORTHY
AND OLIVER B. FRINGER



ABSTRACT. The subject of internal waves interacting with bottom topographic features in the ocean has received much attention in the past few decades. This heightened interest is mainly due to a conjecture that breaking internal waves at boundaries can be a significant source of turbulence, leading to mixing and transport in the ocean. In this paper, we present results from high-resolution three-dimensional numerical simulations of an internal wave interacting with a shelf break in a linearly stratified fluid in order to highlight the instabilities that contribute to wave breaking over topography. The results show the development of a nonlinear internal bolus (a vortex core of dense fluid) that moves upslope as a result of the interaction and subsequent breaking of the internal wave. We present details of the different stages of the interaction process that lead to wave breakdown and formation of internal boluses and their subsequent evolution toward smaller scales of motion and turbulence as they propagate onshore.

INTRODUCTION

The ubiquitous presence of internal waves in the ocean has long been recognized; however, over the last few decades, there has been a significant resurgence of interest in internal waves, mainly due to a proposition that instabilities and breaking internal waves can be a significant source of turbulence and diapycnal (across density surfaces) mixing in the ocean (Munk, 1966; Armi, 1978; Munk and Wunsch, 1998). Indeed, evidence from many open-ocean experiments supports the conjecture that the oceanic internal wave field is the only serious candidate for the supply of energy for diapycnal mixing (Kunze and Toole, 1997; Polzin et al., 1997; Ledwell et al., 1998; Gregg et al., 1999).

Research on internal waves can be classified into three broad categories: (1) generation, (2) propagation and interaction, and (3) dissipation and turbulent mixing. Excellent reviews that provide insightful perspectives into these pieces abound (e.g., Garrett and Munk, 1979; Müller et al., 1986; Thorpe, 2004). At the bottom end of this chain of processes are the small-scale instabilities and wave breaking that lead to

dissipation and turbulent mixing. Mixing can take place in the ocean interior through wave-wave interactions that lead to parametric instabilities and critical layers. In addition to direct interior mixing, internal waves reflecting off topography can lead to energetic mixing due to localized wave breaking that is several orders of magnitude greater than that arising in the open ocean (Alford et al., 2011). The mixed fluid is then advected and stirred into the oceanic interior (Ivey and Nokes, 1989). As such, several studies have been conducted with the goal of understanding small-scale processes that can transfer energy from tidal (barotropic) flows to baroclinic tides and higher-frequency nonlinear internal waves (hereinafter referred to as NLIWs) such as internal solitary waves (ISWs), solibores, and internal boluses, and, ultimately, to turbulent mixing (Apel et al., 1985; Ostrovsky and Stepanyants, 1989; Sandstrom and Oakey 1995; Klymak and Moum, 2003; Carter et al., 2005).

Despite the large amount of existing research on turbulent mixing resulting from internal waves, much remains to be discovered, especially with regard to the structure and ultimate fate (dissipation and mixing) of NLIWs. For example, Klymak and Moum (2003) observed a sequence of three NLIWs of elevation over Oregon's continental shelf, but little is known about how they form, how far onshore they propagate, and how they dissipate. More importantly, robust (dynamic) parameterizations of internal wave dissipation, for use in large-scale ocean general circulation models where such small-scale processes are not explicitly resolved, are still a subject of active research (e.g., Hosegood et al., 2004). This situation can be mainly attributed to the incomplete state of knowledge on the dynamics and fate of NLIWs and the inherent difficulty in modeling turbulence.

The research described in this article was motivated in part by the desire to explain the mechanisms that form nonlinear propagating features on coastal shelves. Although a number of field measurement campaigns document their existence (e.g., Klymak and Moum, 2003; Hosegood et al., 2004; Carter et al., 2005), little is known about their formation or the physics governing their propagation. In particular, due to their strongly nonlinear nature, it is not clear whether these features are solitary waves or gravity currents. Such NLIWs are thought to be prime candidates for transporting mass and sediment (Hosegood

Subhas K. Venayagamoorthy (vskaran@colostate.edu) is Assistant Professor, Department of Civil and Environmental Engineering, Colorado State University, Fort Collins, CO, USA. **Oliver B. Fringer** is Associate Professor, Department of Civil and Environmental Engineering, Stanford University, Stanford, CA, USA.

et al., 2004). Here, a solitary wave can be defined as a wave of permanent form that maintains its structure through a balance between dispersion that tends to broaden its crest and nonlinear effects that tend to steepen it. By contrast, gravity currents appear when fluid of one density propagates (intrudes) into another fluid of different density.

In this article, we build on our previously published results (Venayagamoorthy and Fringer, 2007) from highly resolved three-dimensional numerical simulations of a vertical

mode-1 internal wave interacting with a critical slope (i.e., the wave characteristic slope matches the topographic slope). The new aspects that are addressed in this paper focus on the instabilities that occur in the slope region as well as on the shelf. We present details of the different stages of the interaction process that leads to wave breakdown and formation of vortex cores (or internal boluses) and their subsequent evolution toward smaller scales of motion and turbulence as they propagate onshore.

PROBLEM SETUP AND COMPUTATIONAL APPROACH

The well-known Navier–Stokes equations for conservation of momentum and the continuity equation for conservation of mass govern the behavior of a fluid. These equations, in conjunction with the density transport equation, were solved using the large-eddy simulation (LES) code developed by Fringer and Street (2003) in the computational domain shown in Figure 1 (the lateral width $W = 0.5$ m). This code employs the fractional-step method of Zang et al. (1994) using a finite-volume (control volume) formulation on a curvilinear coordinate (boundary-fitted) grid with a rigid lid (see Figure 1b).

A linear background density stratification is imposed as shown in the schematic in Figure 1, with the Brunt–Väisälä (or buoyancy) frequency $N = 0.57$ rad s^{-1} in a depth of $D = 60$ cm. At the left end of the domain shown in Figure 1, a vertical mode-1 internal wave given by

$$u(0, z, t) = U_0 \cos(mz) \sin(\omega t)$$

is imposed. Note that this relationship implies normal incidence of the wave on the topography and hence ignores any alongshore (y) variation in the incoming wave. Here, U_0 is the velocity amplitude of the forcing, m is the vertical wavenumber corresponding to a mode-1 internal wave with $m = \pi/D$, ω is the forcing frequency, and u is the cross-shore velocity component. It is worth noting here that for an internal wave mode impinging on a slope, it can be shown that the presence of the slope effectively decouples the modal structure of the incident wave into wave beams (Thorpe and Haines, 1987; Thorpe, 1999). Hence, in a continuously stratified

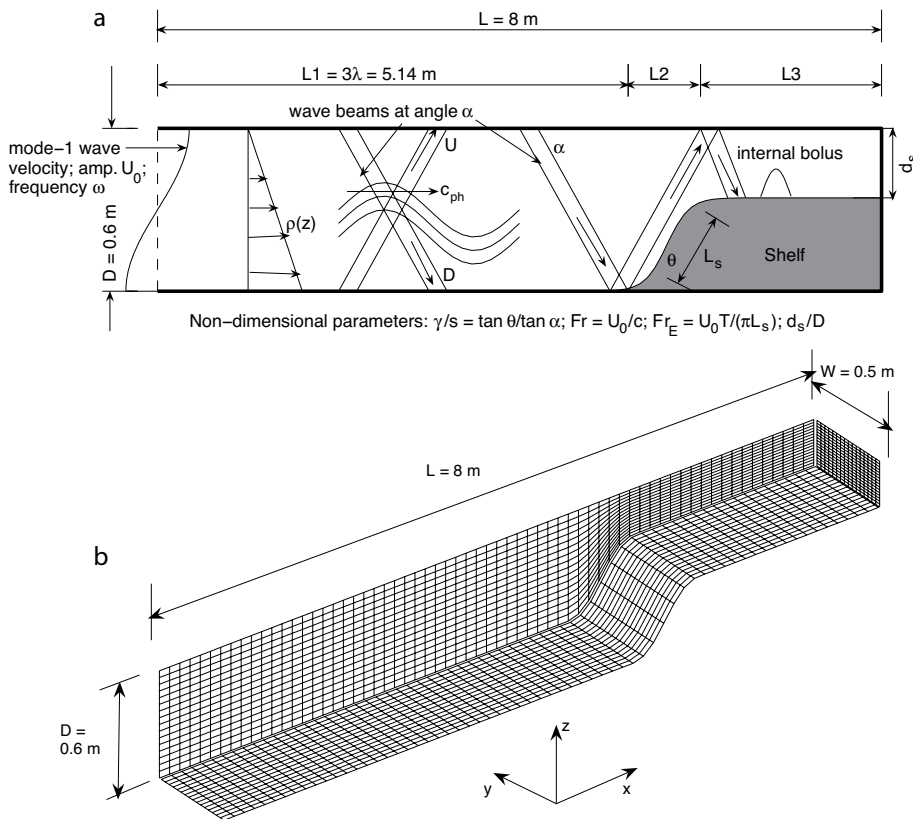


Figure 1. (a) Schematic depicting the computational domain and setup used in the simulations for this study. A mode-1 internal wave is imposed at the left boundary of the domain with a frequency $\omega = 0.33$ rad s^{-1} and wavelength $\lambda = 2\pi/k = 1.713$ m. The topographic slope angle θ is chosen such that it is critical for the given wave frequency. The topographic slope length is $L_s = D = 0.6$ m, which implies that when $\theta = \pi/2$, the reflection coefficient will be 1, and therefore there will be no internal boluses. The schematic also shows the decomposition of the wave mode into a pair of upward (U) and downward (D) propagating wave beams. For clarity, only the reflection of the downward-propagating beam is extended to the slope region. (b) The three-dimensional computational grid used to discretize the domain shown in (a). Every eighth grid cell is plotted for clarity.

fluid of finite depth, a mode can be described as a superposition of pairs of phase-locked upward- and downward-propagating beams. Therefore, although beams are not apparent (at least visually) in the mode-1 propagation dynamics, the slope of their propagation relative to the topographic slope is an important parameter in the present analysis. Boundary conditions for the cross-shore (horizontal) velocity u are no slip on the bottom boundary, free slip at the top boundary, and no flux (gradient-free) at the right boundary. The vertical velocity has a no-flux boundary condition at both top and bottom boundaries and free-slip boundary conditions on all other walls. The grid size is $512 \times 32 \times 128$ for the three-dimensional simulations. A rough estimate of the Kolmogorov turbulence dissipation microscale is about 1 mm using a characteristic length scale of

5 cm, a characteristic velocity scale of $U_0 = 4 \text{ cm s}^{-1}$, and a kinematic viscosity of $\nu = 10^{-5} \text{ m}^2 \text{ s}^{-1}$ (which is higher in the simulations to increase the size of the Kolmogorov scale). With a longitudinal grid spacing of 15 mm, and vertical grid spacing of 5 mm in the deep region and 1.6 mm in the shallow region, the longitudinal grid spacing is about 15 times larger than the Kolmogorov microscale, and the largest vertical grid spacing is five times larger.

WAVE-SLOPE INTERACTION AND FORMATION OF INTERNAL BOLUSES

Figure 2 depicts the interaction of an incoming highly nonlinear mode-1 internal wave with a critical slope (i.e., when $\tan \theta / \tan \alpha = 1$, see Figure 1) using a time sequence of density isosurfaces (or isopycnals, which are

constant density surfaces). As Figure 2a shows, the isopycnals steepen, which leads to wave breaking, causing the isopycnals to fold up, resulting in the formation of a sharp front around which the wave overturns (see Figure 2a,b). These results are consistent with observations made in laboratory experiments of internal waves interacting with slopes by Dauxois et al. (2004) and Ivey and Nokes (1989). Soon after, the overturned lump of fluid surges upslope as the flow oscillates back onshore (Figure 2c). The strong distortion (heaving) of isopycnals leads to wave breaking and formation of dense vortex cores. The surging bolus of fluid travels over the shelf break and is propelled onto the shelf as depicted in Figure 2d as a blob of dense fluid, hereafter referred to as an internal bolus. This bolus then propagates shoreward (see Figure 2e,f) and slowly dissipates

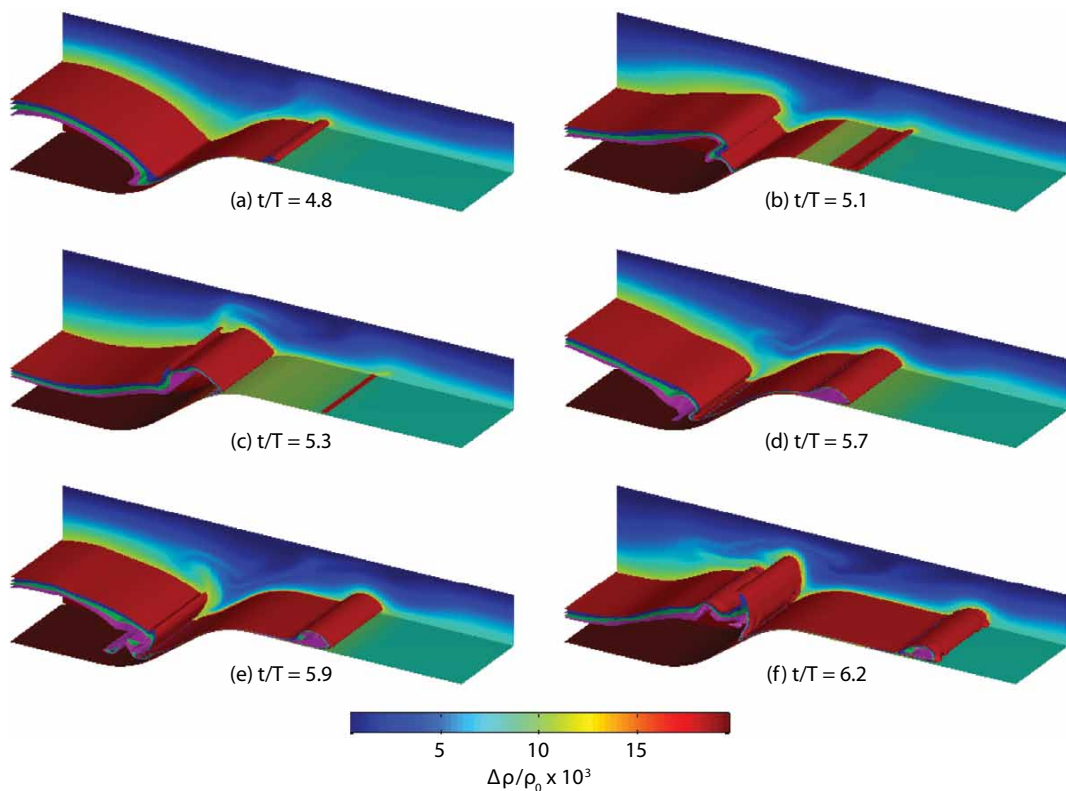


Figure 2. Three-dimensional density isosurfaces of a nonlinear mode-1 internal wave interacting with a critical shelf slope. For clarity, only the right half of the domain from $x = 4.6$ to 6.9 m is shown and time is normalized by the wave period $T = 19.2 \text{ s}$. The isosurface values are $\Delta\rho/\rho_0 = 0.0115$ (red), 0.0125 (blue), 0.0135 (green), and 0.0145 (magenta), and the sideline plane shows the density field as indicated by the color bar.

due to further instabilities (see discussion that follows).

Figure 3 shows a time sequence of an internal bolus that propagates onshelf as a result of the wave-slope interaction process depicted in Figure 2. At time $t/T = 6.0$ (also at earlier times—not shown), the bolus is essentially two dimensional. In Figure 3b, some lateral instabilities begin to develop, and they propagate across the bolus further in time, as Figure 3c and d show, respectively. These instabilities are strikingly similar to the lobe and cleft instabilities observed in gravity current experiments, suggesting that the initial instability that occurs at the bolus front might be three dimensional (Simpson, 1972, 1997). Furthermore, through the use of gravity current scaling (Maxworthy

et al., 2002), Venayagamoorthy and Fringer (2007) determined that these features propagate more like gravity currents than solitary waves.

TYPES OF INSTABILITIES THAT LEAD TO WAVE BREAKING

Many types of instability can be triggered when waves interact with topography. The two most important are:

1. *Static (convective) instability* results from the presence of heavy fluid over light fluid, which leads to overturning (i.e., a local vertical density gradient > 0). Static instability is usually diagnosed using either the value of the local buoyancy frequency N , or the ratio of the local fluid velocity U to the wave phase speed c . Static instability can occur when $N^2 < 0$ or when

$U/c > 1$. Physically, these criteria imply that the isopycnals are locally vertical (that is, opposing gravity; (Koudella and Staquet, 2006).

2. *Dynamic (shear) instability* occurs when the destabilizing effect of high-velocity shear overwhelms the stabilizing effect of density stratification. A classic example is the well-known Kelvin-Helmholtz billows that occur at fluid interfaces such as the oceanic thermocline or in atmospheric shear layers.

It is mostly conjectured that both convective and shear instabilities can occur when internal waves break. A non-dimensional parameter that provides a measure of the importance of buoyancy forces to inertial forces is the local gradient Richardson number defined as

$$Ri_g = \frac{N^2}{(\partial U / \partial z)^2}$$

It has been shown that for steady inviscid parallel stably stratified shear flows, $Ri_g < 0.25$ is a necessary but not sufficient condition for instability to develop from small disturbances (Miles, 1961; Howard, 1961; Drazin, 1977). There are many differing arguments on the applicability of the critical Richardson number criterion $Ri_c = 0.25$ for internal waves. Abarbanel et al. (1984) argue that a local value of $Ri_g < 1$ should suffice to identify regions susceptible to dynamic instability, while Barad and Fringer (2010) argue that $Ri_g < 0.1$ is a sufficient condition for instability in internal solitary waves. In this study, the traditional value of 0.25 is used as a benchmark for evaluating the type of instabilities that develop as a result of the wave-slope interaction process.

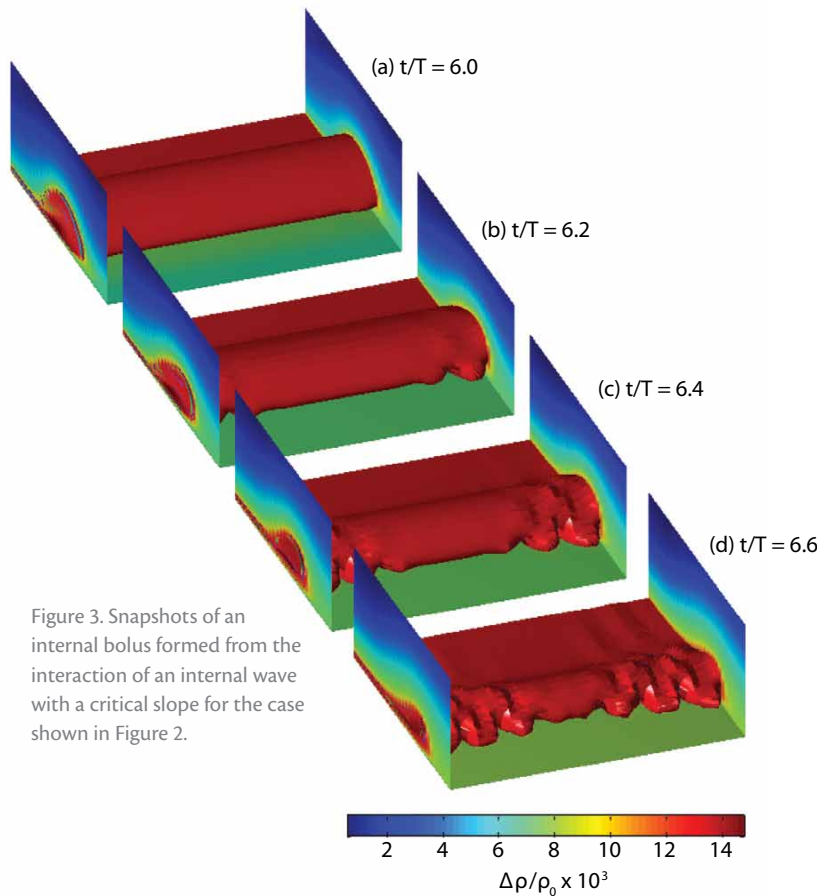


Figure 3. Snapshots of an internal bolus formed from the interaction of an internal wave with a critical slope for the case shown in Figure 2.

INSTABILITY AND BREAKING IN THE SLOPE REGION

Overturning and wave breaking are qualitatively evident in the time sequence plots of the density isosurfaces shown in Figure 2. As Figure 4 shows, the density contours through the middle vertical x - z plane indicate significant distortion and overturning of isopycnals. The sequence depicts wave breaking and formation of upslope surging vortex cores of dense fluid that are ejected onto the shelf as propagating internal boluses as discussed earlier. A better perspective emerges from the contours of the local gradient Richardson number Ri_g . Figure 5A shows contours of $0 \leq Ri_g \leq 0.25$, and Figure 5b shows $Ri_g \leq 0$. The Ri_g values close to the slope are below the critical threshold of 0.25 as seen in Figure 5A. These plots

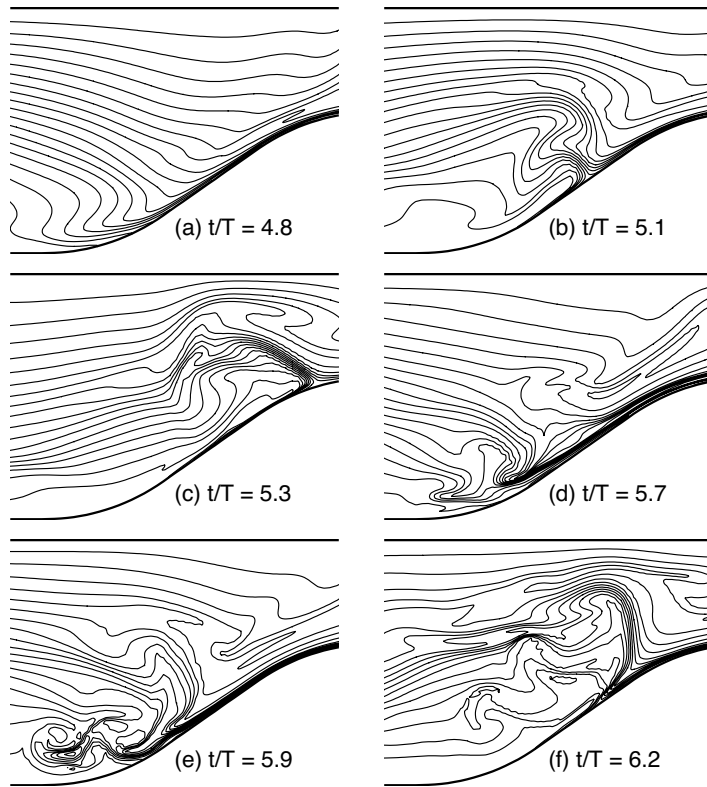


Figure 4. Density contours in the slope region at the middle vertical x - z plane for the case shown in Figure 2. Time is normalized by the wave period $T = 19.2$ s. Contours of density are plotted every 0.2%.

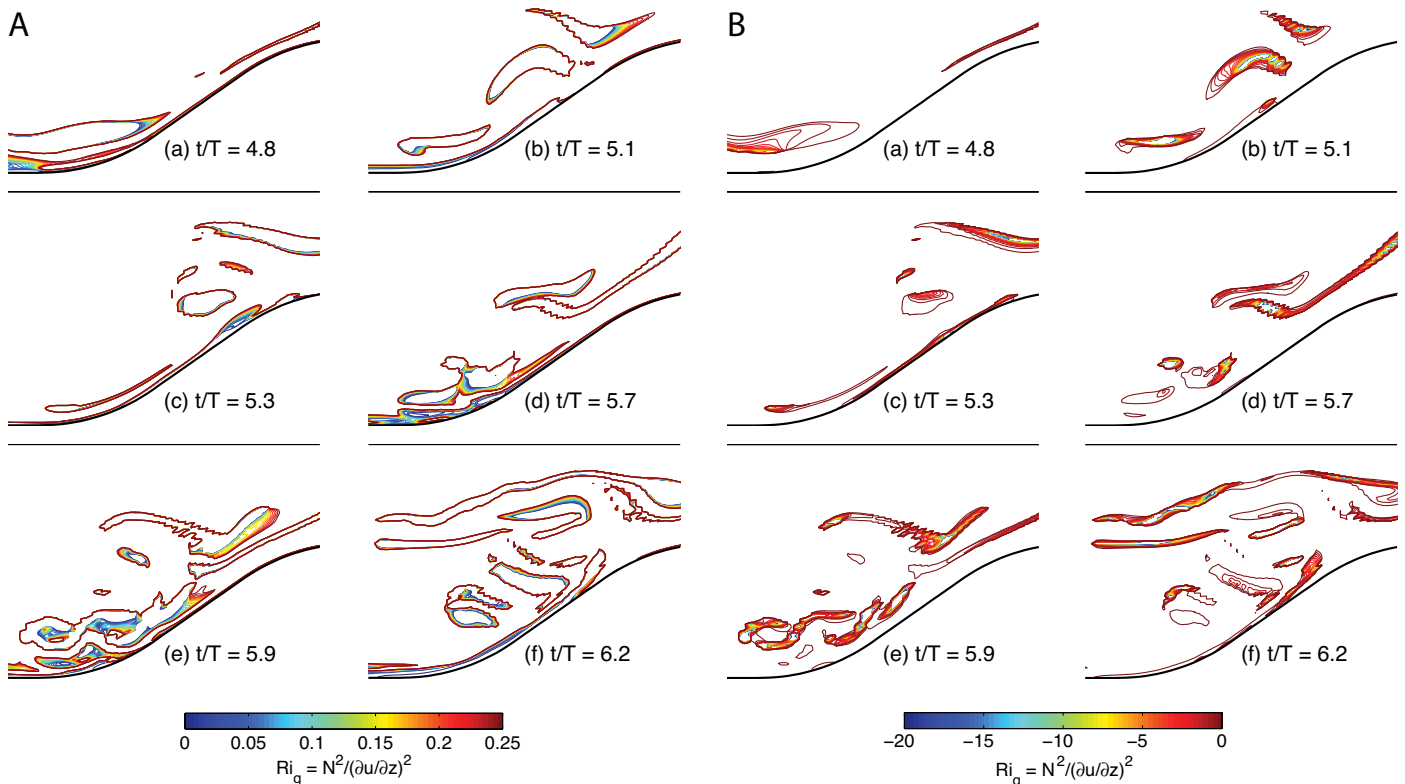


Figure 5. Contours of the local gradient Richardson number for (A) $0 \leq Ri_g \leq 0.25$, and (B) $Ri_g \leq 0$, at the middle vertical x - z plane for the case shown in Figure 2. Time is normalized by the wave period $T = 19.2$ s.

also show that statically unstable regions (i.e. regions with $Ri_g \leq 0$ or equivalently negative values of N^2) are surrounded by regions with small positive values of Ri_g . It is clear from these plots that the regions with $0 \leq Ri_g \leq 0.25$ are very thin. These thin regions surround regions with $Ri_g \leq 0$, implying that there is a transition from stable to unstable stratification. The exceptions to this scenario are the regions close to the bottom boundary (e.g., see the top left, middle right, and bottom left panels of Figure 5A), where regions with $0 \leq Ri_g \leq 0.25$ do not surround a $Ri_g \leq 0$ region. From this qualitative assessment, it can be argued that static instability, associated with overturning, is the instability mechanism above the topography, while in the sheared bottom boundary layer, dynamic (shear) instability is the dominant mechanism.

STRUCTURE OF INTERNAL BOLUSES ONSHELF


The internal boluses that propagate onshelf transport dense fluid. A typical snapshot of an internal bolus as depicted in Figure 6a shows a striking resemblance to the head of a gravity current flowing over a no-slip lower boundary (e.g., see Simpson, 1972; Simpson and Britter, 1979). The nose of the bolus is raised slightly above the bottom wall where the flow is at rest due to the no-slip bottom boundary condition. Figure 6b shows the occurrence of a stagnation point at the nose in a reference frame moving with the wave. Streamline patterns (not shown here) reveal two circulation regions (also visible in Figure 6b) within the bolus. The first is a more pronounced circulation in the upper part of the bolus where circulation speeds have been found to be of order the nose propagation speed

(Venayagamoorthy and Fringer, 2007). The second is a smaller reverse circulation region that occurs close to the lower boundary and causes dense fluid to drain from the bolus.

SUMMARY

Recent observations reveal the presence of nonlinear internal waves in the ocean, but there is a great deal of uncertainty about their structures, how they are generated, and how they propagate and dissipate. This detailed study shows how internal waves interacting with sloping boundaries can lead to the formation of internal boluses onshelf. We presented results from highly resolved three-dimensional numerical simulations of the interaction of mode-1 internal waves with a shelf slope. The focus of this study was to obtain improved understanding of the interaction dynamics at the slope leading to the formation of upslope-surging vortex cores of dense fluid that are eventually ejected onshelf as internal boluses. Examination of the local gradient Richardson number Ri_g indicates that wave breaking may be initiated through a combination of enhanced shear in the bottom boundary layer and static instability associated with wave overturning above the topography.

ACKNOWLEDGEMENTS

The authors gratefully acknowledge the support provided by the Office of Naval Research under grant N00014-05-1-0294 (Scientific Officers: C. Linwood Vincent, Terri Paluszkiwicz, and Scott Harper). 

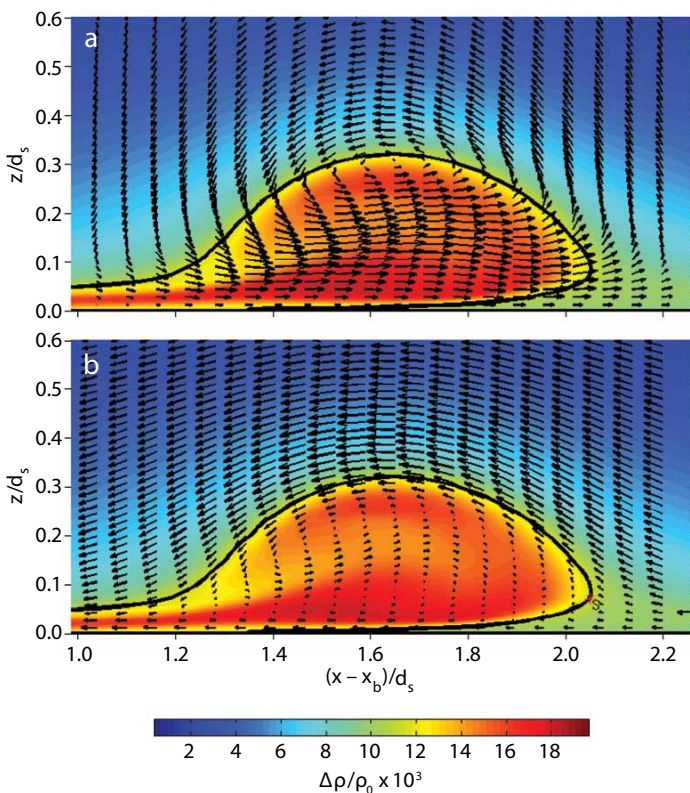


Figure 6. Velocity vectors superimposed on the density contours of an internal bolus in (a) a stationary reference frame to highlight the amplification of onshore velocities at bolus locations onshelf, and (b) a frame that moves to the right at the wave speed. Frame (b) highlights the circulation regions within the core of the bolus. All distances have been normalized by the shelf water depth d_s .

REFERENCES

- Abarbanel, H., D. Holm, J. Marsden, and T. Ratiu. 1984. Richardson number criterion for the non-linear stability of three-dimensional stratified flow. *Physical Review Letters* 52:2,352–2,355, <http://dx.doi.org/10.1103/PhysRevLett.52.2352>.
- Alford, M.H., J.A. MacKinnon, J.D. Nash, H. Simmons, A. Pickering, J.M. Klymak, R. Pinkel, O. Sun, L. Rainville, R. Musgrave, and others. 2011. Energy flux and dissipation in Luzon Strait: Two tales of two ridges. *Journal of Physical Oceanography* 41:2,211–2,222, <http://dx.doi.org/10.1175/JPO-D-11-073.1>.
- Apfel, J.R., J.R. Holbrook, A.K. Liu, and J.J. Tsai. 1985. The Sulu Sea internal soliton experiment. *Journal of Physical Oceanography* 15:1,625–1,651, [http://dx.doi.org/10.1175/1520-0485\(1985\)015<1625:TSSISE>2.0.CO;2](http://dx.doi.org/10.1175/1520-0485(1985)015<1625:TSSISE>2.0.CO;2).
- Armi, L. 1978. Some evidence for boundary mixing in the deep ocean. *Journal of Geophysical Research* 83:1,971–1,979, <http://dx.doi.org/10.1029/JC083iC04p01971>.
- Barad, M.F., and O.B. Fringer. 2010. Simulations of shear instabilities in interfacial gravity waves. *Journal of Fluid Mechanics* 644:61–95, <http://dx.doi.org/10.1017/S0022112009992035>.
- Carter, G.S., M.C. Gregg, and R.-C. Lien. 2005. Internal waves, solitary waves, and mixing on the Monterey Bay shelf. *Continental Shelf Research* 25:1,499–1,520, <http://dx.doi.org/10.1016/j.csr.2005.04.011>.
- Dauxois, T., A. Didier, and E. Falcon. 2004. Observation of near-critical reflection of internal waves in a stably stratified fluid. *Physics of Fluids* 16:1,936–1,941, <http://dx.doi.org/10.1063/1.1711814>.
- Drazin, P.G. 1977. On the instability of an internal gravity wave. *Proceedings of the Royal Society of London A* 356:411–432, <http://dx.doi.org/10.1098/rspa.1977.0142>.
- Fringer, O.B., and R.L. Street. 2003. The dynamics of breaking progressive interfacial waves. *Journal of Fluid Mechanics* 494:319–353, <http://dx.doi.org/10.1017/S0022112003006189>.
- Garrett, C., and W. Munk. 1979. Internal waves in the ocean. *Annual Review of Fluid Mechanics* 11:339–369, <http://dx.doi.org/10.1146/annurev.fl.11.010179.002011>.
- Gregg, M.C., D.W. Winkel, J.A. MacKinnon, and R.C. Lien. 1999. Mixing over shelves and slopes. Pp. 35–42 in *Internal Wave Modeling*. P. Müller and D. Henderson, eds. *Proceedings of the Aha Hulikoà Hawaiian Winter Workshop*.
- Hosegood, P., J. Bonnin, and H. van Haren. 2004. Solibore-induced sediment resuspension in the Faeroe-Shetland Channel. *Geophysical Research Letters* 31, L09301, <http://dx.doi.org/10.1029/2004GL019544>.
- Howard, L. 1961. Note on a paper of John W. Miles. *Journal of Fluid Mechanics* 10:509–512, <http://dx.doi.org/10.1017/S0022112061000317>.
- Ivey, G.N., and R.I. Nokes. 1989. Vertical mixing due to the breaking of critical internal waves on sloping boundaries. *Journal of Fluid Mechanics* 204:479–500, <http://dx.doi.org/10.1017/S0022112089001849>.
- Klymak, J.M., and J.N. Moum. 2003. Internal solitary waves of elevation advancing on a shoaling shelf. *Geophysical Research Letters* 30(20), 2045, <http://dx.doi.org/10.1029/2003GL017706>.
- Koudella, C.R., and C. Staquet. 2006. Instability mechanisms of a two-dimensional progressive internal gravity wave. *Journal of Fluid Mechanics* 548:165–196, <http://dx.doi.org/10.1017/S0022112005007524>.
- Kunze, E., and J.M. Toole. 1997. Tidally driven vorticity, diurnal shear, and turbulence atop Fieberling Seamount. *Journal of Physical Oceanography* 27:2,663–2,693, [http://dx.doi.org/10.1175/1520-0485\(1997\)027<2663:TDVDSA>2.0.CO;2](http://dx.doi.org/10.1175/1520-0485(1997)027<2663:TDVDSA>2.0.CO;2).
- Ledwell, J.R., A.J. Watson, and C.S. Law. 1998. Mixing of a tracer in the pycnocline. *Journal of Geophysical Research* 103(C10):21,499–21,529, <http://dx.doi.org/10.1029/98JC01738>.
- Maxworthy, T., J. Leulich, J.E. Simpson, and E. Meiburg. 2002. The propagation of a gravity current into a linearly stratified fluid. *Journal of Fluid Mechanics* 453:371–394, <http://dx.doi.org/10.1017/S0022112001007054>.
- Miles, J. 1961. On the stability of heterogeneous shear flows. *Journal of Fluid Mechanics* 10:496–508, <http://dx.doi.org/10.1017/S0022112061000305>.
- Müller, P., G. Holloway, F. Henyey, and N. Pomphrey. 1986. Nonlinear interactions among internal gravity waves. *Reviews of Geophysics* 24:493–536, <http://dx.doi.org/10.1029/RG024i003p00493>.
- Munk, W. 1966. Abyssal recipes. *Deep-Sea Research* 13:707–730, [http://dx.doi.org/10.1016/0011-7471\(66\)90602-4](http://dx.doi.org/10.1016/0011-7471(66)90602-4).
- Munk, W., and C. Wunsch. 1998. Abyssal recipes II: Energetics of tidal and wind mixing. *Deep-Sea Research Part I* 45:1,977–2,010, [http://dx.doi.org/10.1016/S0967-0637\(98\)00070-3](http://dx.doi.org/10.1016/S0967-0637(98)00070-3).
- Ostrovsky, L.A., and Y.A. Stepanyants. 1989. Do internal solitons exist in the ocean? *Reviews of Geophysics* 27:293–310, <http://dx.doi.org/10.1029/RG027i003p00293>.
- Polzin, K.L., J.M. Toole, J.R. Ledwell, and R.W. Schmitt. 1997. Spatial variability of turbulent mixing in the abyssal ocean. *Science* 276:93–96, <http://dx.doi.org/10.1126/science.276.5309.93>.
- Sandstrom, H., and N.S. Oakey. 1995. Dissipation in internal tides and solitary waves. *Journal of Physical Oceanography* 25:604–614, [http://dx.doi.org/10.1175/1520-0485\(1995\)025<0604:DIITAS>2.0.CO;2](http://dx.doi.org/10.1175/1520-0485(1995)025<0604:DIITAS>2.0.CO;2).
- Simpson, A.E. 1972. Effects of the lower boundary on the head of a gravity current. *Journal of Fluid Mechanics* 53:759–768, <http://dx.doi.org/10.1017/S0022112072000461>.
- Simpson, A.E. 1997. *Gravity Currents*. Cambridge University Press, 262 pp.
- Simpson, A.E., and R.E. Britter. 1979. The dynamics of the head of a gravity current advancing over a horizontal surface. *Journal of Fluid Mechanics* 94:477–495, <http://dx.doi.org/10.1017/S0022112079001142>.
- Thorpe, S.A., and A.P. Haines. 1987. On the reflection of a train of finite-amplitude internal waves from a uniform slope. *Journal of Fluid Mechanics* 178:279–302, <http://dx.doi.org/10.1017/S0022112087001228>.
- Thorpe, S.A. 1999. The generation of alongslope currents by breaking internal waves. *Journal of Physical Oceanography* 29:29–45, [http://dx.doi.org/10.1175/1520-0485\(1999\)029<0029:TGOACB>2.0.CO;2](http://dx.doi.org/10.1175/1520-0485(1999)029<0029:TGOACB>2.0.CO;2).
- Thorpe, S.A. 2004. Recent developments in the study of ocean turbulence. *Annual Review of Earth and Planetary Sciences* 32:91–109, <http://dx.doi.org/10.1146/annurev.earth.32.071603.152635>.
- Venayagamoorthy, S.K., and O.B. Fringer. 2007. On the formation and propagation of nonlinear internal boluses across a shelf break. *Journal of Fluid Mechanics* 577:137–159, <http://dx.doi.org/10.1017/S0022112007004624>.
- Zang, Y., R.L. Street, and J.R. Koseff. 1994. A non-staggered grid, fractional step method for time-dependent incompressible Navier-Stokes equations in curvilinear coordinates. *Journal of Computational Physics* 114:18–33, <http://dx.doi.org/10.1006/jcph.1994.1146>.